

2. Ohkuwa M, Hosokawa K, Boku A, et al. New endoscopic treatment for intramucosal gastric tumors using an insulated-tip diathermic knife. *Endoscopy* 2001;33:221-6.
3. Hosokawa K, Yoshida S. Recent advances in endoscopic mucosal resection for early gastric cancer [Japanese with English abstract]. *Jpn J Cancer Chemother* 1998;25:476-83.
4. Gotoda T, Kondo H, Ono H, et al. A new endoscopic mucosal resection (EMR) procedure using an insulation-tipped diathermic (IT) knife for rectal flat lesions. *Gastrointest Endosc* 1999;50:560-3.
5. Oyama T, Kikuchi Y. Aggressive endoscopic mucosal resection in the upper GI tract: Hook knife EMR method. *Minim Invasive Ther Allied Technol* 2002;11:291-5.
6. Yahagi N, Fujishiro M, Kakushima N, et al. Endoscopic submucosal dissection for early gastric cancer using the tip of an electrosurgical snare (thin type). *Dig Endosc* 2004;16:34-8.
7. Yamamoto H, Kawata H, Sunada K, et al. Successful en bloc resection of large superficial tumors in the stomach and colon using sodium hyaluronate and small-caliber-tip transparent hood. *Endoscopy* 2003;35:690-4.
8. Oka S, Tanaka S, Kaneko I, et al. Advantage of endoscopic submucosal dissection compared with EMR for early gastric cancer. *Gastrointest Endosc* 2006;64:877-83.
9. Röscher T, Sarbia M, Schmacher B, et al. Attempted endoscopic en bloc resection of mucosal and submucosal tumors using insulated-tip knives: a pilot series. *Endoscopy* 2004;36:788-801.
10. Choi U, Kim CG, Chang HJ, et al. The learning curve for EMR with circumferential mucosal incision in treating intramucosal gastric cancer. *Gastrointest Endosc* 2005;62:860-5.
11. Gotoda T, Friedland S, Hamanaka H, et al. A learning curve for advanced endoscopic resection. *Gastrointest Endosc* 2005;62:866-7.
12. Matsushita M, Hajiro K, Okazaki K, et al. Endoscopic mucosal resection of gastric tumors located in the lesser curvature of the upper third of the stomach. *Gastrointest Endosc* 1997;45:512-5.
13. Kobayashi T, Gotoda T, Tamakawa K, et al. Magnetic anchor for more effective endoscopic mucosal resection. *Jpn J Clin Oncol* 2004;34:118-23.
14. Gotoda T. A large endoscopic resection by endoscopic submucosal dissection (ESD) procedure. *Clin Gastroenterol Hepatol* 2005;3:571-3.
15. Soetikno R, Gotoda T, Nakanishi Y, et al. Endoscopic mucosal resection. *Gastrointest Endosc* 2003;57:567-9.
16. Ludwig K, Klautke G, Bernhard J, et al. Minimally invasive and local treatment for mucosal early gastric cancer. *Surg Endosc* 2005;19:1362-6.
17. Deyhle P, Largiader F, Jenny P. A method for endoscopic electroresection of sessile colonic polyps. *Endoscopy* 1973;5:38-40.
18. Tada M, Murakami A, Karita M, et al. Endoscopic resection of early gastric cancer. *Endoscopy* 1993;25:445-51.
19. Gotoda T. Endoscopic resection of early gastric cancer: the Japanese perspective. *Curr Opin Gastroenterol* 2006;22:561-9.
20. Inoue H, Takeshita K, Hori H, et al. Endoscopic mucosal resection with a cap-fitted panendoscope for esophagus, stomach, and colon mucosal lesions. *Gastrointest Endosc* 1993;39:58-62.
21. Akiyama M, Ota M, Nakajima H, et al. Endoscopic mucosal resection of gastric neoplasms using a ligating device. *Gastrointest Endosc* 1997;45:182-6.
22. Korenaga D, Haraguchi M, Tsujitani S, et al. Clinicopathological features of mucosal carcinoma of the stomach with lymph node metastasis in eleven patients. *Br J Surg* 1986;73:431-3.
23. Ell C, May A, Gossner L, et al. Endoscopic mucosectomy of early cancer and high-grade dysplasia in Barrett's esophagus. *Gastroenterology* 2000;118:670-7.
24. Tanabe S, Koizumi W, Mitomi H, et al. Clinical outcome of endoscopic aspiration mucosectomy for early stage gastric cancer. *Gastrointest Endosc* 2002;56:708-13.
25. Eguchi T, Gotoda T, Oda I, et al. Is endoscopic one-piece mucosal resection essential for early gastric cancer? *Dig Endosc* 2003;15:113-6.
26. Gotoda T, Sasako M, Ono H, et al. An evaluation of the necessity of gastrectomy with lymph node dissection for patients with submucosal invasive gastric cancer. *Br J Surg* 2001;88:444-9.
27. Gotoda T, Yanagisawa A, Sasako M, et al. Incidence of lymph node metastasis from early gastric cancer: estimation with a large number of cases at two large centers. *Gastric Cancer* 2000;3:219-25.
28. Etoh T, Katal H, Fukagawa T, et al. Treatment of early gastric cancer in the elderly patient: results of EMR and gastrectomy at a national referral center in Japan. *Gastrointest Endosc* 2005;62:868-71.
29. Soetikno R, Kaltenbach T, Yeh R, et al. Endoscopic mucosal resection for early cancers of the upper gastrointestinal tract. *J Clin Oncol* 2005;23:4490-8.
30. Ohashi S. Laparoscopic intraluminal surgery for early gastric cancer: is it a new concept in laparoscopic intraluminal surgery. *Surg Endosc* 1995;9:169-71.
31. Ohgami M, Otani Y, Kumai K, et al. Curative laparoscopic surgery for early gastric cancer: five years experience. *World J Surg* 1999;23:187-93.
32. Kondo H, Gotoda T, Ono H, et al. Percutaneous traction-assisted EMR by using an insulation-tipped electrosurgical knife for early stage gastric cancer. *Gastrointest Endosc* 2004;59:284-8.
33. Faddis MN, Blume W, Finney J, et al. Novel, magnetically guided catheter for endocardial mapping and radiofrequency catheter ablation. *Circulation* 2002;106:2980-5.
34. Zeltser IS, Bergs R, Fernandez R, et al. Single trocar laparoscopic nephrectomy using magnetic anchoring and guidance system in the porcine model. *J Urol* 2007;178:288-91.
35. Scott DJ, Tang SJ, Fernandez R, et al. Completely transvaginal NOTES cholecystectomy using magnetically anchored instruments. *Surg Endosc* 2007;21:2308-16.

Received December 7, 2007. Accepted March 31, 2008.

Current affiliations: Endoscopy Division (T.G., I.O.), National Cancer Center Hospital, Tokyo, Tamakawa Corporation (K.T.), Sendai, Pentax Corporation (H.U.), Tokyo, Cancer Screening Technology Division (T. Kobayashi), Research Center for Cancer Prevention and Screening, National Cancer Center (T. Kakizoe), Tokyo, Japan.

Reprint requests: Takuji Gotoda, MD, Endoscopy Division, National Cancer Center Hospital, 5-1-1 Tsukiji, Chuo-ku, Tokyo 104-0045, Japan.

If you want to chat with an author of this article, you may contact him at tgotoda@ncc.go.jp.

Cantilevered actuator using magnetostrictive thin film

Kazushi Ishiyama*, Chikako Yokota

Research Institute of Electrical Communication, Tohoku University, 2-1-1 Katahira Aoba, Sendai 980-8577, Japan

Available online 6 April 2008

Abstract

This paper describes a cantilevered magnetic actuator driven by magnetostriction in a low magnetic field. The dimensions of the two layers actuator were 1×5 mm and amorphous FeSiB was used as the magnetostrictive material. Since the FeSiB has excellent soft magnetic characteristics, the actuator with FeSiB was able to work in magnetic field strength of less than 10 kA/m. The theoretical formulas for the amount of the displacement and the force of the actuator were obtained. The theoretical results agreed with the experimental one. According to the theoretical formula, the displacement was calculated with the parameter of the mechanical properties of the substrate. To obtain the large displacement, the actuator with Co substrate was designed based on the theoretical formula. The displacement of 153 μ m was obtained using Cu substrate of 1.1 μ m thickness in the magnetic field of 10 kA/m. © 2008 Elsevier B.V. All rights reserved.

© 2008 Elsevier B.V. All rights reserved.

PACS: 75.50.Kj; 75.80.+q; 85.85.+j

Keywords: Cantilever; FeSiB; Magnetostriction; Magnetic thin film; Low magnetic field

1. Introduction

Cantilevered actuators were studied using principles of piezoelectric effect [1], thermal expansion [2], and magnetostriction [3]. Using the piezoelectric effect and thermal expansion, the large displacement can be obtained. However, the structures are complicated because they require insulation layers and signal cables. In this study, we proposed a cantilevered actuator driven by magnetostriction. The actuator can drive wirelessly, and the structure is simple. Therefore, the actuator is suitable for miniaturization. In previous works, amorphous TbFe and SmFe thin films were studied for the magnetostrictive materials for the actuator, because they had large magnetostriction constant [3]. However, a large magnetic field of about 80–800 kA/m was required to drive, and it was not suitable for the application in microsystems.

In this work we fabricated the cantilevered actuator using amorphous FeSiB as magnetostrictive material. This material has smaller magnetostriction constant of about

30×10^{-6} compared with rare earth iron alloys, but has large permeability. Therefore this material is suitable for magnetostrictive cantilever in low magnetic field less than 10 kA/m. The theoretical formulas about the amount of the displacement and the force of the actuator were obtained. According to the theoretical formula, the displacement was calculated with the parameter of the mechanical properties of the substrate. The actuator was designed for Young's modulus and the thickness of the substrate, to obtain the largest displacement.

2. Cantilevered magnetic actuator

2.1. Driving principle

The shape of the magnetostrictive material expands or contracts by the rotation of the magnetic moment in the material. The amorphous FeSiB and a non-magnetic material were made up of the two-layer cantilever actuator. Not to receive the influence of a magnetic torque, the magnetic field was applied to the width direction of the actuator. Because the amorphous FeSiB has a positive magnetostriction constant, the FeSiB film contracts to

*Corresponding author. Tel.: +81 22 217 5488; fax: +81 22 217 5728.
E-mail address: ishiyama@iec.tohoku.ac.jp (K. Ishiyama).

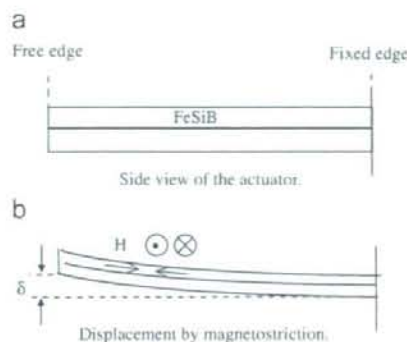


Fig. 1. Configuration and displacement of the magnetic actuator. (a) Side view of the actuator. (b) Displacement by magnetostriction.

transverse direction of the applied magnetic field. Therefore the cantilever bends toward the FeSiB side. The side view of the actuator is shown in Fig. 1(a). By applying an external magnetic field as shown in Fig. 1(b) the actuator bends. The displacement δ and the force F were observed at the free edge of the actuator.

2.2. Fabrication and measurement of the actuator

The amorphous FeSiB thin films were fabricated by the RF sputtering method. The sputtering target was Fe₇₂Si₁₄B₁₄ alloy. RF input power was 200 W, and Ar gas pressure was controlled to obtain the best residual stress. During the sputtering, the substrate was cooled by water. The thickness of the FeSiB was 0.7 μm . After deposition, the magnetic film was cut out to 1 \times 5 mm with the substrate. We defined it as the cantilevered actuator. To control the magnetic anisotropy, the actuator was heat treated in the magnetic field of 240 kA/m to the longitudinal direction of the cantilever and the temperature of 350 $^{\circ}\text{C}$ in 1 h. The magnetic characteristics were measured using VSM. The amount of the displacement of the actuator in magnetic field 10 kA/m was measured by microscope, and the force was measured by microscope with loads at the free edge of the cantilever. The weights of the loads were measured with the weight meter, with accuracy of μg order beforehand.

3. Derivation of the theoretical formulas

3.1. Displacement

The various theoretical formulas about the amount of the displacement of cantilevered actuator by the magnetostriction have been studied [4,5]. However, the theoretical formulas are suitable only for that the magnetic film is thin enough compared to the substrate. Therefore, it is necessary to obtain a new theoretical formula for this research, because we have to apply very thin substrate for large displacement [6].

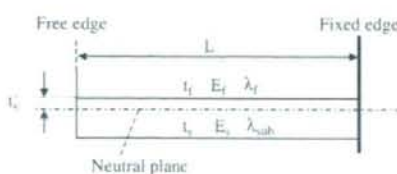


Fig. 2. Structure of the cantilevered actuator and neutral plane.

A neutral plane was defined as shown in Fig. 2. This was the plane in the actuator whose length was not changed when the actuator bends. The distance between the neutral plane and contact plane of the layers was defined as t'_s . The theoretical formula was obtained by using t'_s and the following two assumptions. The bending moment diagram was the same at the total length of the actuator, and the bending angle of the actuator was small enough compared with the actuator length [7]. The obtained theoretical formulas were shown as follows:

$$t'_s = \frac{E_s t_s^2 - E_f t_f^2}{2(E_s t_s + E_f t_f)} \quad (1)$$

$$\delta = \frac{3L^2 \{E_s \lambda_{\text{sub}} t_s (-t_s + 2t'_s) + E_f \lambda_f t_f (t_f + 2t'_s)\}}{4 \{E_s t_s (t_s^2 - 3t_s t'_s + 3t'^2_s) + E_f t_f (t_f^2 + 3t_f t'_s + 3t'^2_s)\}} \quad (2)$$

where δ is the amount of the displacement in the free edge of the actuator, L is the actuator length, and t_f , E_f , and λ_f are the thickness, Young's modulus, and the magnetostriction of the magnetic thin film, respectively. t_s , E_s , and λ_{sub} are the thickness, Young's modulus, and the magnetostriction of the substrate material, respectively. t'_s is the distance between the neutral plane and contact plane of the layer. In this study, the length L was constant as 5 mm, Young's modulus of the magnetic thin film E_f was 210 GPa.

When the magnetostriction value λ in the theoretical formulas was used, the following two points were considered. The first point was the influences of the relation between the direction of the applied magnetic field and the observation. The magnetic field was applied to the width direction of the actuator in this experiment; the magnetostriction value λ' was converted into $-1/2$ of the magnetostriction constants. The other point is that the magnetic moment was not saturated at the field of 10 kA/m. Under an assumption that the magnetization changed in rotation in FeSiB because it was exited to its hard direction, we used a ratio between saturation magnetization and the magnetization at 10 kA/m. This ratio was multiplied with the magnetization constant to compare with the experimental value in 10 kA/m.

3.2. Force

We examined the force generated at the free edge of the actuator when the magnetic field was applied to the actuator. The force was equal to the concentrated load on the free edge. Under the same assumption as the

Table 1
Calculated and experimental values for the displacement and force of the cantilevered magnetic actuator ($H = 10 \text{ kA/m}$)

Thickness of magnetic thin film, t_f (μm)		0.35	0.70	1.05
Displacement (μm)	Calculated	6.9	7.9	8.3
	Experiment	7.1	8.0	8.4
Force (μN)	Calculated	3.0	4.2	5.0
	Experiment	3.1	4.3	4.9

theoretical formula (2), the theoretical formula about the force of the actuator was obtained as follows.

$$F = \frac{3w\{E_s\lambda_{\text{sub}}t_s(-t_s + 2t'_s) + E_f\lambda_f t_f(t_f + 2t'_s)\}}{4L} \quad (3)$$

where F is the amount of the force in the free edge point of the actuator and, w is the width of the actuator. In this study, the width was constant as 1 mm. Other parameters were the same as those used in theoretical formula (2).

3.3. Experiment and comparison with theory

As shown in Table 1, the calculated values of the displacement and the force agreed well with the experimental results using a polyimide film as the non-magnetic substrate. The mechanical properties were used as the following values: t_s : $30 \mu\text{m}$, E_s : 3.5 GPa. The magnetostriction of the film, λ_f , was -15×10^{-6} , because the field was applied to the width direction of the cantilever while the length was changed by the magnetostriction. From the results shown in Table 1, it is found that the formulas are suitable to design the actuator.

4. Design of a cantilever actuator

4.1. Theory analysis of the displacement

Based on the theoretical formula, the amount of the displacement of the actuator was analyzed with the kinds of the substrates. The dimensions of the actuator were $1 \times 5 \text{ mm}$, and the thickness of the FeSiB was $0.7 \mu\text{m}$. The parameters for the analysis were the mechanical properties of the non-magnetic substrate as Young's modulus and the thickness. The analytical results are shown in Fig. 3. The horizontal axis shows the Young's modulus of the substrate, and the vertical axis shows thickness of the substrate, and the numerical value which each lines show is the calculated amount of the displacement of the actuator. The substrate material can be decided according to the relation between Young's modulus and the thickness of the substrate.

It is found that the higher the Young modulus of the substrate obtained, the large the displacement, while there was the optimum value for the thickness, as shown in Fig. 3. If the substrate material had a high Young's modulus, the substrate material strongly disturbed the contraction of the FeSiB magnetostrictive material. On the

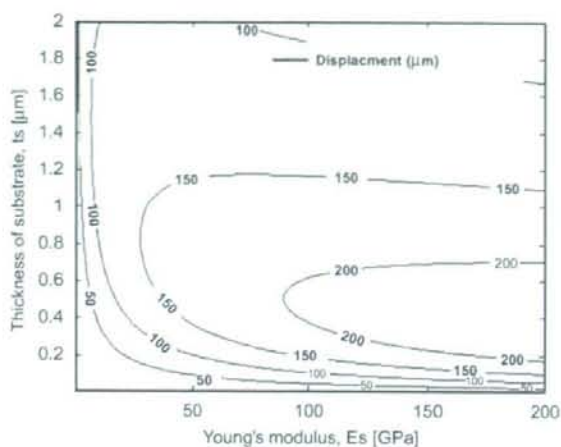


Fig. 3. Figure of the amount of the displacement designed by Young's modulus and the thickness of the substrate.

other hand, a soft and thin substrate would contract with magnetostrictive layer. Therefore, the contraction would not be converted to the large displacement in these conditions. Therefore the best substrate thickness and Young's modulus exist to obtain the large displacement. When the material of Young's modulus 130 GPa was applied for the substrate to obtain the amount of the displacement of about $150 \mu\text{m}$, the thickness of the substrate must be $1.1 \mu\text{m}$. Cu was selected as a substrate material with this Young's modulus, and the calculated displacement value was $155 \mu\text{m}$ under the actuator length of 5 mm.

4.2. Experiment and comparison

Based on the foregoing paragraph, the actuator with the Cu substrate was fabricated. Cu and FeSiB thin films were fabricated by the RF sputtering method. RF input power was 100 W, and Ar gas pressure was 4 mTorr for Cu and 16 mTorr for FeSiB. The annealing temperature was $200 \text{ }^\circ\text{C}$ in consideration of the difference of the coefficient of thermal expansion.

The displacement was measured as shown in Fig. 4. The experimental result shows the displacement of $153 \mu\text{m}$ with the magnetic field strength of 10 kA/m . The obtained experimental result was agreed well with the calculated value.

In addition, the produced force of this actuator was $0.30 \mu\text{N}$ while the calculated value was $0.29 \mu\text{N}$. This result confirms the design was suitable for the cantilever actuator.

It is clarified that we could obtain the cantilevered actuator as we designed and the amount of displacement more than $100 \mu\text{m}$ was obtained. Moreover, the graph showed that the amount of the displacement is almost saturated with magnetic field strength of 10 kA/m , and the influence of hysteresis was hardly seen. These results show

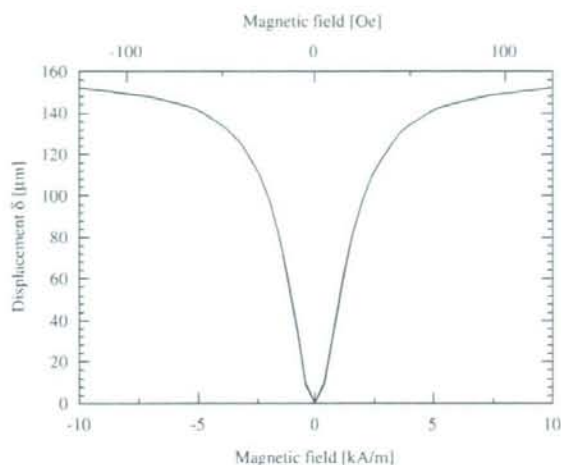


Fig. 4. Experimental result between the magnetic field and the displacement δ caused by the magnetostriction.

that this actuator has the large possibility for the application of the microsystems such as μTAS .

5. Summary

The cantilevered actuator driven by the magnetostriction was examined. The two-layer actuator was made using amorphous FeSiB thin film, so the actuator could be driven in the low magnetic field less than 10 kA/m. The theoretical

formulas for the amount of the displacement and for the force of the actuator were obtained. The calculated values agreed well with the experimental results using a polyimide film as the non-magnetic substrate. To obtain the actuator with large amount of the displacement, Cu film was applied for the substrate, based on the design of the theoretical formula. As the results, the actuator with large displacement was fabricated as designed based on the theoretical formula.

References

- [1] M. Okugawa, Y. Hori, *Trans. Jpn. Soc. Mech. Eng. C* 69 (2003) 858.
- [2] O. Nakabeppu, T. Kanda, *IEEJ Trans. SM* 124 (2004) 453.
- [3] K.I. Arai, T. Honda, *J. Jpn. Soc. Precis. Eng.* 60 (1994) 1699.
- [4] T. Honda, K.I. Arai, *J. Magn. Soc. Jpn.* 21 (1997) 817.
- [5] A.C. Tam, H. Schroeder, *J. Appl. Phys.* 64 (1988) 5422.
- [6] C. Yokota, A. Yamazaki, M. Sendoh, S. Agatsuma, K. Morooka, K. Ishiyama, K.I. Arai, *J. Magn. Soc. Jpn.* 30 (2006) 302.
- [7] Y. Takahashi, S. Machida, *Kisozairyourikigaku (in Japanese)*, Baihukan, Tokyo, 1988, pp. 131.